Journal of Membrane Science 446 (2013) 181–188

Contents lists available at ScienceDirect

Journal of Membrane Science

journal homepage: www.elsevier.com/locate/memsci

Hydrophobic-ZIF-71 filled PEBA mixed matrix membranes for recovery of biobutanol via pervaporation

Sainan Liu, Gongping Liu, Xuhong Zhao, Wanqin Jin*

State Key Laboratory of Materials-Oriented Chemical Engineering, College of Chemistry and Chemical Engineering, Nanjing University of Technology, 5 Xinmofan Road, Nanjing 210009, PR China

ARTICLE INFO

Article history:
Received 2 May 2013
Received in revised form
14 June 2013
Accepted 17 June 2013
Available online 25 June 2013

Keywords:
Mixed matrix membranes
ZIF-71
PEBA
Acetone–butanol–ethanol
Pervaporation

ABSTRACT

As an alternative energy source to fossil fuels, biobutanol has received increasing attention. In this work, new mixed matrix membranes (MMMs) incorporating zeolitic imidazolate frameworks (ZIF-71) particles into polyether-block-amide (PEBA) were prepared for biobutanol recovery from acetone–butanol–ethanol (ABE) fermentation broth by pervaporation (PV). FESEM, EDS, XRD, FT-IR, DSC and contact angle measurements were conducted to study the morphologies, physical and chemical properties and surface properties of the MMMs. The PV performance of the prepared MMMs with various ZIF-71 loadings for separating n-butanol from its aqueous solution was investigated. As a result, both separation factor and thickness-normalized flux of the PEBA membranes were improved by incorporating appropriate amount of ZIF-71 (≤20 wt%). The membrane with 20 wt% ZIF-71 was evaluated in ABE model solution and ABE fermentation broth, and exhibited high n-butanol separation performance. ZIF-71 particles were confirmed as promising fillers to enhance the separation performance for butanol recovery because of their excellent compatibility with polymer and organophilicity. This work demonstrated the ZIF-71/PEBA MMMs could be potential candidates for practical biobutanol production.

1. Introduction

Energy crisis is one of the major global issues due to the shortage of fossil fuels. As an alternative renewable energy resource, biofuel has attracted increasing attention in recent years. Butanol, one of the most valuable biofuels, is mainly produced by acetone–butanol–ethanol (ABE) fermentation from renewable biomass. However, the yield and productivity of ABE fermentation process are low because fermentation is inhibited by the produced butanol [1,2]. In order to eliminate the inhibition, many in-situ product recovery systems including gas stripping, pervaporation, perstraction and adsorption have been developed. Among these methods, pervaporation (PV) is considered to be the greatest potential separation technology because of its energy-saving and efficiency, as well as no harmful effects on the microorganisms [3,4].

Polyether-block-amide (PEBA) comprising flexible polyether and rigid polyamide segments has recently been studied to remove alcohols from water by pervaporation [5–10]. It was found that PEBA has a considerably high affinity to butanol [5]. Moreover, the preparation method for PEBA membranes is very simple: dissolution–casting–evaporation without any crosslinking reaction, polymerization or stretching. These features are beneficial for the industrial application of PEBA membranes. Boddeker [9] and Yen [10] found that PEBA membranes exhibited a higher butanol permeation flux than polydimethylsiloxane (PDMS) membranes. The feasibility of utilizing PEBA membranes for acetone–butanol–ethanol extraction from dilute aqueous solution was demonstrated by Feng [5]. From the previous reported results, the pervaporation performance of PEBA membranes is still not meeting the requirements for practical application.

Mixed matrix membranes (MMMs) composed of porous particle fillers dispersed in a polymeric matrix combine the favorable features of polymers and particle fillers and have been proved to be promising materials for PV separation. Commonly used inorganic particles in alcohols separations include silicalite [8,11], zeolite [12–14], silica [15], and carbonaceous particles [16]. However, these particles filled membranes have some issues which constrain their practical application. The main issue is the incompatibility between the inorganic and polymeric phases, resulting in defects in the membranes. With such defects, the MMMs exhibit little or no improvement in selectivity over the original polymer membranes [17]. Another challenge is that the separation properties of the MMMs generally follow distinct tradeoff relations: the higher selectivity the lower permeability [14].

The recently developed metal organic frameworks (MOFs) comprise metal centers connected by various organic linkers with tunable surface areas and pore volumes [18]. Compared with zeolites, the organic nature of the framework may facilitate

---

* Corresponding author. Tel.: +86 25 83172266; fax: +86 25 83172292.
E-mail address: wqjin@njut.edu.cn (W. Jin).

0376-7388/$ - see front matter © 2013 Elsevier B.V. All rights reserved.
http://dx.doi.org/10.1016/j.memsci.2013.06.025

interactions with the polymer that allow a good compatibility. Therefore, incorporating MOFs into polymeric matrix to prepare MMMs is believed to be a facile way to improve the separation performance of polymeric membranes [19–27]. To date, the studies on MOF-containing MMMs for pervaporation application are still very limited [23,25,26]; especially no studies on biobutanol recovery from real ABE fermentation broth were reported. Different from n-butanol/water mixture, the fermentation broth has not only complex compounds, but also a different density, pH and viscosity. The PV performance and stability of membranes can be diminished in the fermentation broth. Screening of suitable MOF materials to prepare MMMs for butanol recovery from real ABE fermentation broth is a challenge. Zeolitic imidazolate frameworks (ZIFs), a subclass of MOFs show superior thermal and chemical stability and exhibit great promise for a variety of applications [28]. ZIF-71 is a superhydrophobic material [29–31]; therefore the incorporation of the hydrophobic ZIF-71 into PEBA can be expected to enhance the performance for alcohol recovery. In addition, ZIF-71 particles can be synthesized at room temperature [30]. Thus, the preparation of ZIF-71 particles is a lower cost, time-saving, and a much more convenient way compared to the hydrothermal synthesis of zeolites and most of MOFs at high temperature and autogenous pressure.

In this study, for the first time superhydrophobic and organophilic ZIF-71 particles are introduced as fillers to prepare MMMs with the aim of enhancing the separation factor and flux simultaneously. The objective of this study is to explore the ZIF-71/PEBA 2533 mixed matrix membranes for recovery of n-butanol from ABE fermentation broth via pervaporation. The pervaporation separation performance of the MMMs in n-butanol aqueous solution, model ABE solution and ABE fermentation broth was investigated.

2. Experimental

2.1. Materials

PEBA 2533 was purchased from Arkema, France. Acetone and n-butanol were of analytical grade from Shanghai Shenbo Chemical Co., Ltd., China. Methanol and ethanol were purchased from Wuxi City Yasheng Chemical Co., Ltd. Zinc acetate and 4,5-dichloroimidazole (dcIm) were supplied by Alfa Aesar. Poly(vinylidene fluoride) (PVDF) supports (average pore size: 450 nm) were obtained from Solvay, America. All of the materials were used without further purification.

2.2. Synthesis of ZIF-71 crystals

ZIF-71 crystals were synthesized at room temperature using the procedure described in a previous report [30]. A solution of zinc acetate (0.4458 g, 2.40 mmol) in 90 mL of methanol was rapidly poured into a solution of dcIm (1.3152 g, 9.60 mmol) in 90 mL of methanol under stirring. The mixture turned turbid immediately. After stirring at room temperature for 24 h, the crystals were separated by centrifugation and washed with fresh methanol. Then, the particles were dispersed in fresh methanol before use.

2.3. Membrane preparation

ZIF-71 particles were separated by centrifugation from the suspension in methanol and re-dispersed in n-butanol. The ZIF-71/n-butanol suspension was stirred and sonicated alternatively for 1/2 h for three times each. The ZIF-71 crystals were first "primed" [20] by adding a small amount of PEBA (w_{PEBA}:$w_{butanol}$=1.4:93) into the suspension, then it was further stirred at 80 °C for 4 h. Subsequently, the remaining bulk polymer (w_{PEBA}:$w_{butanol}$=5.6:93) was added and stirred for another 4 h. After that, the solution was kept at 60 °C overnight to eliminate trapped air bubbles. Membranes were cast on PVDF substrate by a flat membrane casting equipment. The solvent was evaporated at room temperature for 2 days, and then dried in oven at 70 °C for 24 h. The thickness of the membrane ranged from 10 to 20 μm.

2.4. ABE fermentation

2.4.1. Culture and inoculum preparation

Clostridium acetobutylicum XY16 (China Center for Type Culture Collection, CCTCC NO: M 2010011) was used in all experiments. Cells were grown in 50 mL sealed anaerobic bottles containing 25 mL seed medium with the following composition: soluble starch 10 g/L, yeast extract 3 g/L, peptone 5 g/L, ammonium acetate 2 g/L, sodium chloride 2 g/L, KH_2PO_4 1 g/L, K_2HPO_4 1 g/L, $MgSO_4$ 3 g/L and $FeSO_4 \cdot 7H_2O$ 0.01 g/L. The medium was autoclaved at 121 °C for 15 min and cooled to 37 °C. Anaerobic bottles were inoculated with 1 mL of a −70 °C glycerol stock culture and incubated at 37 °C for 20–24 h as the primary seed culture. Before inoculation, nitrogen was bubbled through the medium for 1 min to remove oxygen. 7.5 mL of the primary seed culture was inoculated into 250 mL sealed anaerobic bottles containing 150 mL of seed medium and incubated at 37 °C for 12 h as the secondary seed culture. Before inoculation, nitrogen was bubbled through the medium for 3 min to remove oxygen.

2.4.2. Fermentation

Batch fermentation was conducted in a 2 L serum bottle (Boeco, Germany). The fermentation medium contained: glucose 60 g/L, ammonium acetate 2.2 g/L, corn steep liquor (CSL) 1 g/L, sodium chloride 0.01 g/L, KH_2PO_4 0.5 g/L, K_2HPO_4 0.5 g/L, $MgSO_4$ 0.2 g/L, $MnSO_4 \cdot 7H_2O$ 3 g/L and $FeSO_4 \cdot 7H_2O$ 0.01 g/L. The pH was set at 6.8 using 5 M NaOH. The fermentor containing 1.5 L fermentation medium was autoclaved at 121 °C for 15 min and cooled under oxygen-free nitrogen gas atmosphere to 37 °C for 20 min in clean bench area, then 150 mL of the secondary seed culture was inoculated into fermentor. The fermentation was run at 37 °C for 72 h. The resulted fermentation broth was used as the feed for pervaporation.

2.5. Pervaporation measurement

The pervaporation experiment was conducted on a homemade apparatus [14]. The flat membrane was sealed in a stainless steel PV cell. The feed solution was maintained at a preset temperature and circulated between the feed tank and the membrane cell with a flow rate of 12 L/h. The permeate vapor was collected in liquid nitrogen trap. The pressure at permeate side was below 400 Pa during collections. Acetone, butanol and ethanol concentrations were determined by gas chromatography (GC-2014, Shimadzu, Japan).

The PV performance of a membrane is usually expressed in terms of the flux J, separation factor β and pervaporation separation index (PSI). To eliminate the effect of the membrane thickness on flux, thickness-normalized flux J' (normalized to 100 μm) is also used.

$$J = \frac{W}{At} \tag{1}$$

$$J' = \frac{W}{At} \times \frac{l}{100} \tag{2}$$

$$\beta_i = \frac{Y_i/(1-Y_i)}{X_i/(1-X_i)} \tag{3}$$

$$\mathrm{PSI} = J(\beta-1) \tag{4}$$

where W is the weight of the permeate, A the effective area of the membrane and t the permeation time interval for the pervaporation and l the membrane thickness; Y_i and X_i are the weight fractions of component i in the permeate and feed, respectively.

Since the flux is dependent on the operating conditions, normalizing the flux with respect to the driving force for permeation is useful to further understand the permeant-specific intrinsic membrane properties changed [14] by the incorporation of ZIF-71 particles into PEBA membrane. This intrinsic membrane property is the permeability P and selectivity α, which are defined based on the solution-diffusion mechanism.

$$\frac{W_i}{t} = \frac{P_i A(p_{i,feed}^{vapour} - n_{i,permeate} p_{permeate})}{l} \tag{5}$$

$$\alpha^i_{H_2O} = \frac{P_i}{P_{H_2O}} \tag{6}$$

where W_i is the partial permeate weight of component i, l the membrane thickness, $p_{i,feed}^{vapour}$ the equilibrium partial vapor pressure of i in the feed, $n_{i,permeate}$ the mole fraction of i in the permeate and $p_{permeate}$ the permeate pressure; P_i and P_{H_2O} are the permeabilities of component i and water, respectively.

2.6. Characterization

Adsorption and desorption isotherms for n-butanol and water with ZIF-71 particles were obtained using an Intelligent Gravimetric Analyzer (IGA, IGA-100, Hiden analytical). The morphologies of ZIF-71, PVDF supported PEBA and ZIF-71/PEBA membranes were examined by field emission scanning electron microscope (FESEM, S4800, Hitachi). Energy dispersive spectrometry (EDS) elemental mapping was taken using an energy dispersion of X-ray system equipped with a window connected to a FESEM S4800 operating at 20 kV. Fourier Transform infrared spectroscopy (FT-IR, Nicolet8700, Nicolet) spectra were recorded in spectrophotometer with the range of 1800–600 cm^{-1}, using the KBr disk technique. Thirty-two scans were accumulated with a resolution of 2 cm^{-1} for each spectrum. The crystal structures of ZIF-71 and the membranes were characterized by X-ray diffractometer (XRD, Bruker, D8 Advance) using Cu Kα radiation, in the range of 2–40° with an increment of 0.02° at room temperature. The static contact angles of these membranes were measured by the Sessile drop method using contact angles measurement system (DSA100, Kruss) at room temperature. The average contact angle was obtained by measuring the same sample at three different sites. Differential scanning calorimetry (DSC, Q2000 V24.9 Build 121) measurements were carried out from −100 °C to 20 °C in N_2 atmosphere.

3. Results and discussion

3.1. ZIF-71 particle property

The morphology of ZIF-71 particles is shown in Fig. 1. The crystals do not display a distinct morphology and can be described as cubic with the average particle size of approximately 1 μm.

Adsorption and desorption isotherms for butanol and water vapor with ZIF-71 particles were measured at 40 °C. As shown in Fig. 2, butanol vapor uptake into ZIF-71 exhibits a Type V isotherm, indicating that the adsorption interaction is weak, and the n-butanol could be easily desorbed. Similar adsorption–desorption hysteresis on ZIF-71 has been observed for other alcohols [30]. In contrast, water uptake into ZIF-71 is very low and no capillary condensation point was observed in the tested pressure range, indicating that the ZIF-71 has high hydrophobicity. Because of the hydrogen bonds, water can hardly break in the bulk phase and be adsorbed in the hydrophobic cage. However, n-butanol exhibits a large amount of adsorption even at low pressures. The hydrophobicity and organophilicity of ZIF-71 are attributed to its stronger affinity to less polar n-butanol than water [29].

3.2. Membrane characterization

3.2.1. Morphology

ZIF-71/PEBA MMMs were prepared by incorporating ZIF-71 particles into PEBA. For comparison, Fig. 3a and b shows the FESEM

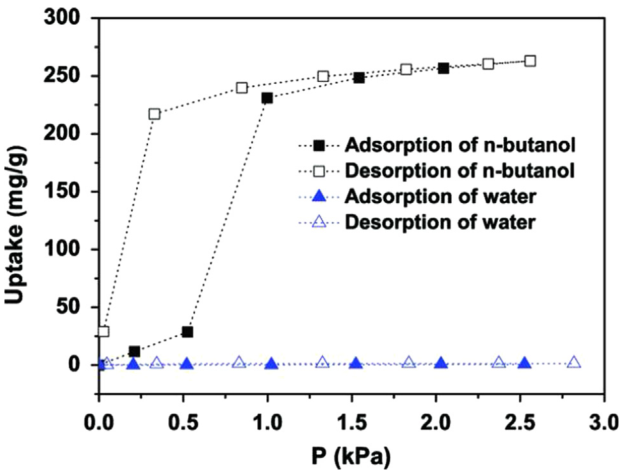

Fig. 2. Adsorption and desorption isotherms for n-butanol and water with ZIF-71 at 40 °C.

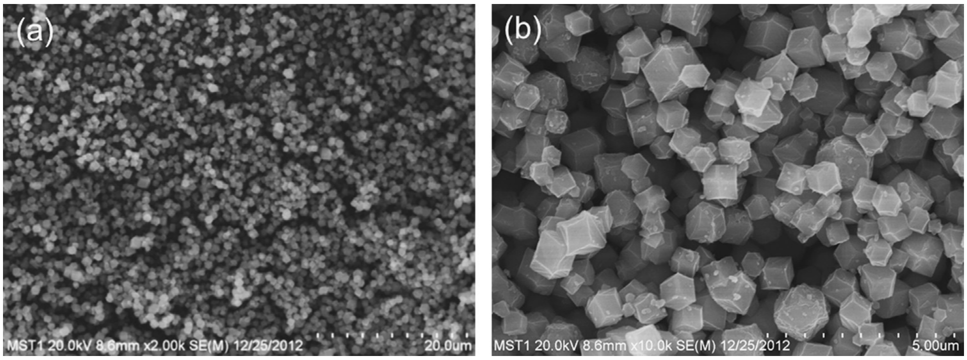

Fig. 1. FESEM images of (a) ZIF-71 crystals and (b) ZIF-71 crystals with higher magnification.

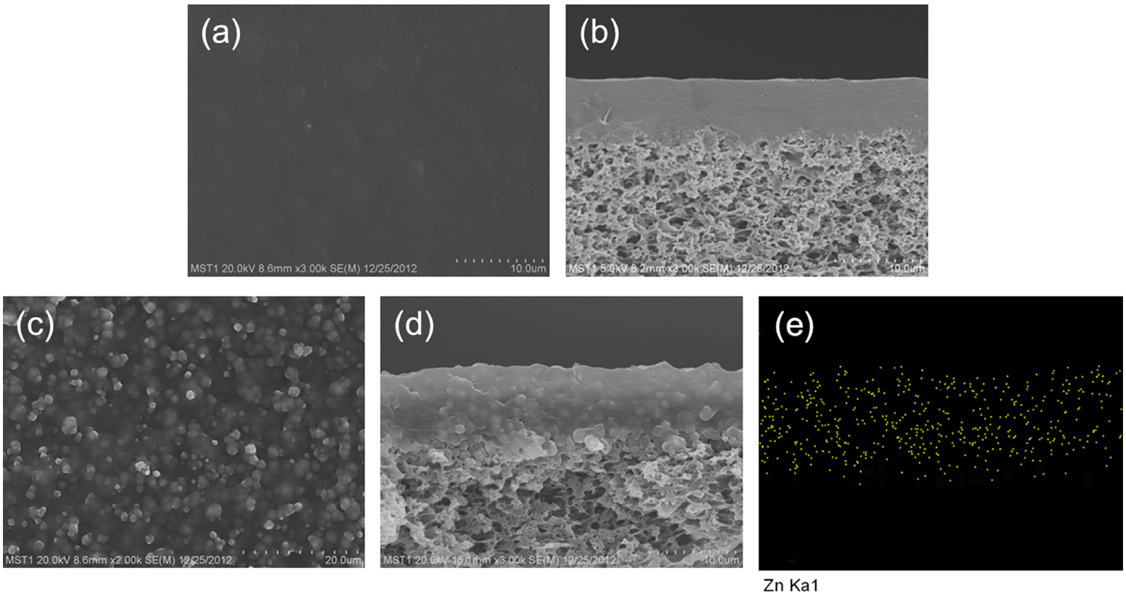

Fig. 3. FESEM images of the (a) surface (b) and cross-section of PEBA membrane; (c) surface and (d) cross-section of ZIF-71/PEBA MMMs with ZIF-71 loading of 25 wt%; and (e) EDS mapping of ZIF-71/PEBA MMMs with ZIF-71 loading of 25 wt% (Zn signal: yellow). (For interpretation of the references to color in this figure legend, the reader is referred to the web version of this article.)

images of the PVDF supported pure PEBA composite membrane. The active PEBA layer is uniformly coated on the supports. The surface of the composite membrane is dense and defect-free (Fig. 3a), and membrane structures could be observed clearly (Fig. 3b). The PEBA layer adheres well to the support layer. For preparing the ZIF-71/PEBA MMMs, ZIF-71 particles were synthesized in methanol and then separated by centrifugation from the suspension and re-dispersed in n-butanol to overcome particle agglomeration. Without performing the conventional drying procedure, the interactions between the particles can be avoided [22]. Thus, the particles can be distributed homogeneously in PEBA without agglomeration. Meanwhile, a thin PEBA coating was introduced onto the surface of ZIF-71 by adding a little PEBA polymer into the solution. This “primed” [20] coating prevented particles from agglomeration and reduced interphase voids in the mixture. FESEM images of the surface and cross-section of the membrane with 25 wt% loading are shown in Fig. 3c and d. The incorporated ZIF-71 particles are closely embedded in PEBA phase, without interfacial voids and agglomeration. The cross section morphology and EDS mapping (Fig. 3e) show that ZIF-71 particles were homogeneously distributed in PEBA polymeric matrix.

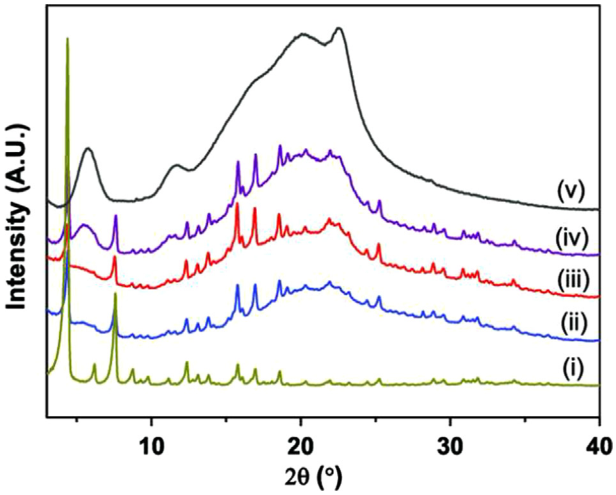

Fig. 4. XRD spectra of (i) ZIF-71; (ii) ZIF-71/PEBA MMMs with 10 wt% loading; (iii) ZIF-71/PEBA MMMs with 20 wt% loading; (iv) ZIF-71/PEBA MMMs with 25 wt% loading; and (v) pure PEBA membrane.

3.2.2. *Structures*

The XRD patterns of ZIF-71 and ZIF-71/PEBA MMMs are shown in Fig. 4. The broad peak of pure PEBA membrane indicates that it is amorphous at room temperature. The diffraction patterns of the ZIF-71/PEBA MMMs suggest that the polymer matrix does not alter the structure of ZIF-71. The ZIF-71 structure becomes obvious with increasing ZIF-71 loading.

The FT-IR spectra of the PEBA, ZIF-71 and ZIF-71/PEBA MMMs were presented in Fig. 5. For PEBA membrane, the band at 1640 cm^{-1} is attributed to the stretching vibration of the H–N–C=O group. The peak at 1100 cm^{-1} is assigned to the stretching vibration of C–O–C group. For the ZIF-71/PEBA MMMs, the intensity of bands at 665 cm^{-1} (vibration of C–Cl) and 1055 cm^{-1} (vibration of C–N) increases with increasing the ZIF-71 loading. No apparent shifts in the bands were observed for the MMMs.

The glass transition temperature (T_g) is an important thermal parameter to estimate the chain flexibility or rigidity of polymer materials. Table 1 lists the T_g values of the pristine PEBA membrane and ZIF-71/PEBA MMMs with different loading. With the increase of ZIF-71 loading, T_g firstly decreases and then increases. The decrease of T_g is resulted from that the addition of a small amount of ZIF-71 particles could disrupt the inherent organization of the polymer chains, and enhance the accessible free volume in the matrix. The T_g of MMMs with 10 wt% loading is very close to that with 20 wt%. Nevertheless, when the incorporation of ZIF-71 reaches 25 wt%, the T_g increases obviously. This may be caused by partial chain rigidification of the polymer matrix with high weight loading [7].

3.2.3. *Surface contact angle analysis*

The pervaporation performance of a membrane for alcohol recovery is related to the organophilicity and hydrophobicity of

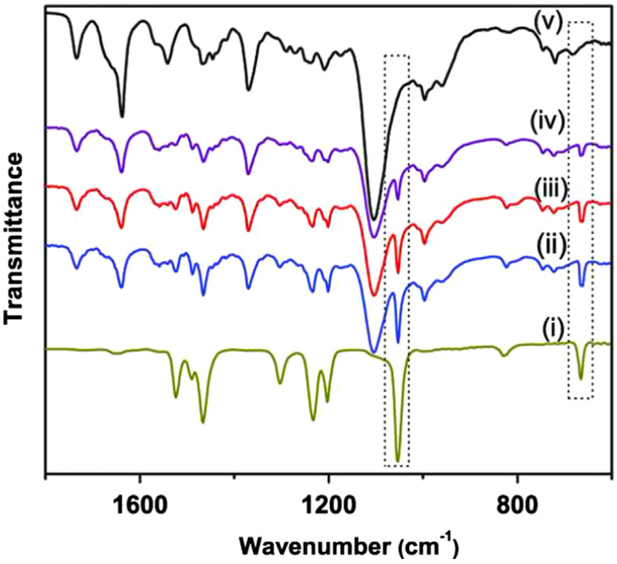

Fig. 5. FT-IR spectra of (i) ZIF-71; (ii) ZIF-71/PEBA MMMs with 10 wt% loading; (iii) ZIF-71/PEBA MMMs with 20 wt% loading; (iv) ZIF-71/PEBA MMMs with 25 wt% loading; and (v) pure PEBA membrane.

Table 1
T_g of ZIF-71/PEBA MMMs with different loading.

Membrane	T_g (°C)
PEBA	−73.88
MMMs with 10 wt% loading	−76.00
MMMs with 20 wt% loading	−75.55
MMMs with 25 wt% loading	−74.35

the separation layer. Generally, the surface property of membrane can be described by the contact angles. The surface organophilicity of the ZIF-71/PEBA MMMs was evaluated by n-butanol static contact angles measurements and the results are shown in Table 2. With increasing ZIF-71 loading, the butanol contact angles decreased from 18.0° to 10.3°, indicating that the incorporation of ZIF-71 enhanced the affinity between n-butanol and the membranes. The low butanol contact angles indicate the high solubility of butanol in the membranes. The hydrophobic property of membranes was tested by water contact angles. The results show that the ZIF-71 filled PEBA membranes were more hydrophobic than the unfilled membranes. It is attributed to the hydrophobic nature of ZIF-71, as well as the increased surface roughness caused by the introduction of ZIF-71 particles. In addition, the water static contact angles show that the surface of the membranes are not highly hydrophobic. Therefore, the membranes would not be fouled easily in the fermentation broth [32].

3.3. PV performance of ZIF-71/PEBA MMMs

3.3.1. PV performance in binary n-butanol–water mixture

Fig. 6 shows the effect of ZIF loading on the performance of ZIF-71/PEBA MMMs for butanol recovery from a 1 wt% n-butanol aqueous solution. The thickness-normalized flux firstly increases and then declines with increasing the loading, reaching the maximum value at 20 wt% loading. In contrast, the separation factor increases with the loading, and the maximum separation factor of 22.3 is achieved at 25 wt% loading. In order to further understand the intrinsic membrane properties changed by the incorporation of ZIF-71 particles, the fluxes (n-butanol and water) were normalized to permeabilities by taking into the account the driving forces for permeation and membrane thickness.

Table 2
Butanol and water contact angles of the ZIF-71/PEBA MMMs with different loading.

Membrane	Butanol contact angles (deg)	Water contact angles (deg)
PEBA	18.0	67.5
MMMs with 10 wt% loading	16.3	70.2
MMMs with 20 wt% loading	13.5	74.1
MMMs with 25 wt% loading	10.3	84.5

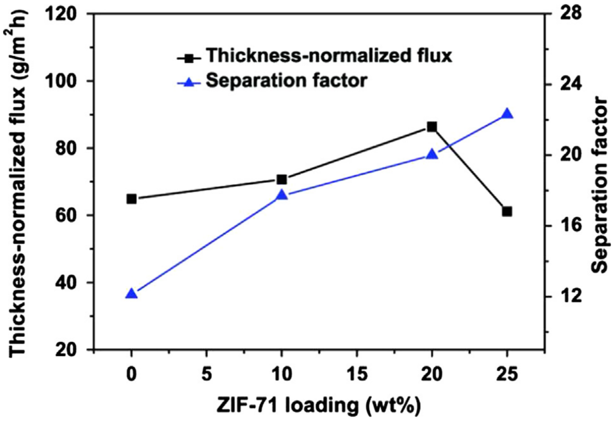

Fig. 6. Effect of ZIF-71 loading on the separation factor and total thickness-normalized flux of the ZIF-71/PEBA MMMs. Temperature: 40 °C and feed concentration: 1 wt% n-butanol.

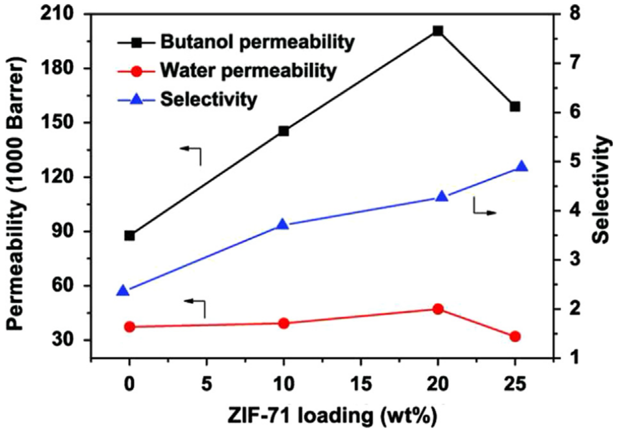

Fig. 7. Effect of ZIF-71 loading on the permeate permeability and selectivity of the ZIF-71/PEBA MMMs. Temperature: 40 °C and feed concentration: 1 wt% n-butanol (1 barrer = 1×10^{-10} cm^3(SPT)cm^{-2} s^{-1} cm Hg^{-1}).

The effect of ZIF-71 loading on permeability (n-butanol and water) and selectivity of the MMMs was investigated. As displayed in Fig. 7, the incorporation of ZIF-71 could firstly increase and then decrease both the n-butanol and water permeability, and the highest permeability is achieved at 20 wt% loading. With low ZIF-71 loading, the chain packing of the MMMs is more loose than the pure PEBA membrane, which is proved by the T_g data. In addition, butanol molecules can diffuse freely though the pores of the ZIF-71 cages because of the flexible frameworks and "gate opening" effect of ZIF-71 with 0.48 nm windows and big cages (1.68 nm) [31]. Both of the factors lead to the increase of butanol permeability in the MMMs. However, when the incorporation of ZIF-71 reached 25 wt%, partial chain rigidification of the polymer matrix occurs as confirmed by T_g. Moreover, higher amount of particles could result in higher transport resistance due to the tortuous pathways across the membrane. Thus, the butanol and water permeabilities decreased with ZIF-71 loading above 20 wt%.

The selectivity increases with ZIF-71 loading, and reaches 4.88 at the loading of 25 wt%, which is two times of the unfilled PEBA membrane. It can be speculated from the permeabilities of n-butanol and water that the increase of $P_{butanol}$ is more rapid than P_{water} when the ZIF loading is lower than 20 wt%. Both the more loose chain packing of the MMMs and hydrophobic inner channel of ZIF-71 could increase $P_{butanol}$, while only the former contributes to the increase of P_{water}. In addition, more loose chain packing can improve diffusivity selectivity for a larger molecule [33] (n-butanol). With the loading above 20 wt%, the P_{water} and $P_{butanol}$ both decreased because of partial chain rigidification; however, n-butanol could diffuse though the pores of the ZIF-71, resulting in lower decreasing rate of $P_{butanol}$ than P_{water}. Therefore, the separation factor and selectivity of the MMMs increased with the ZIF loading.

It is worth to note that the separation factor and flux increased synchronously with ZIF-71 loading from 0 to 20 wt%. The unique relationship between separation factor and flux is opposite to the common trade-off limit where an increase in flux is accompanied by a loss in separation factor.

3.3.2. PV performance in model ABE solution

A model solution, consisting of 0.6 wt% of acetone, 1.2 wt% of butanol and 0.2 wt% of ethanol, was prepared to simulate the supernatant of a fermentation broth. The pervaporation performance of ZIF-71/PEBA MMMs with 20 wt% loading was investigated at 37 °C and the experimental results are shown in Table 3. The separation factor and partial flux of the membrane follow the order of n-butanol > acetone > ethanol. The selective permeation of PEBA membrane is primarily due to the preferential sorption. The sorption experiments carried by Feng [5] showed that the solvent uptake in PEBA membrane followed the order of n-butanol > acetone > ethanol. This is in agreement with the separation performance (fractional flux and separation factor) of ABE in the model solution and real fermentation broth. Compared with the total flux of 550.0 g/m^2 h in binary n-butanol–water mixture at 40 °C, the flux in ABE–water model solution is slightly lower because of the lower operation temperature of 37 °C. In addition, the n-butanol separation factor is also lower than that in binary system due to the co-solution of acetone and ethanol and coupling effects among the permeant species because of the permeant–permeant and permeant–membrane interactions [5].

3.3.3. PV performance in ABE fermentation broth

The difference between ABE fermentation broth and the model solution is not only the difference in their density, pH and viscosity, but also the presence or absence of the inactive microbial cells and several other metabolic compounds. The PV performance and stability of ZIF-71/PEBA mixed matrix membrane with 20 wt% loading in the ABE fermentation broth at 37 °C were studied to investigate the effect of typical impermeable components on the membrane performance and the results are shown in Fig. 8. The ABE composition is close to the model solution. The average total flux of 447.9 g/m^2 h in the fermentation broth is lower compared with that in the ABE water solution. The composition of the fermentation broth is complex, including corn steep liquor, inactive microbial cells and other microbial cells, and these components could adsorb on the membrane surface, which hinders the transport of the permeates. However, the effect on the ABE separation factor was negligible compared to the results in ABE solution. The possible explanation is that the microbial cells would not reduce the affinity of the membrane to ABE molecules. Furthermore, the high hydrophobic inner channel surfaces of ZIF-71 also contribute to the selective separation of n-butanol significantly, and these channels will not be influenced by the microbial cells. As shown in Fig. 8, during the 100 h of continuous PV experiment, the performance of ZIF-71/PEBA MMMs is stable, only with little deviation due to the fluctuation of ABE feed concentration. The average total flux is 447.9 g/m^2 h with the average separation factor of acetone, n-butanol and ethanol of 8.8, 18.4 and 3.6, respectively. This stability indicates that, although the inactive cells in the fermentation broth could decrease the total flux, their effects on membrane fouling are not obvious. The interfacial morphology of the composite membrane after the 100 h of continuous PV experiment in ABE fermentation broth is shown in Fig. 9. It can be seen that the ZIF-71/PEBA layer still adheres well to the PVDF support after long term running.

Table 3
PV performance of MMMs with 20 wt% loading in model ABE solution.

	Acetone	n-Butanol	Ethanol	Total
Flux (g/m^2 h)	25.0	96.8	4.2	520.2
Separation factor	8.2	18.8	3.9	15.5

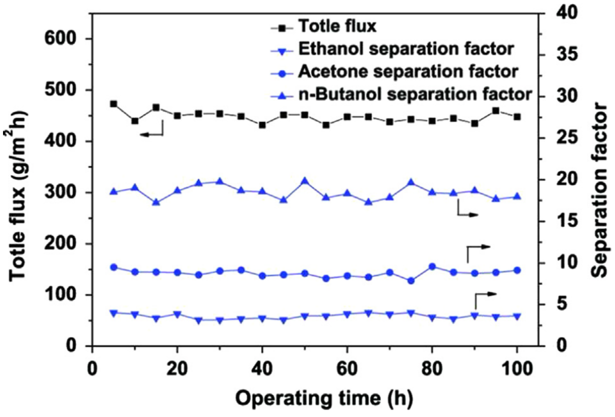

Fig. 8. Stability of ZIF-71/PEBA MMMs with 20 wt% loading in ABE fermentation broth: total flux and separation factor of acetone, n-butanol and ethanol.

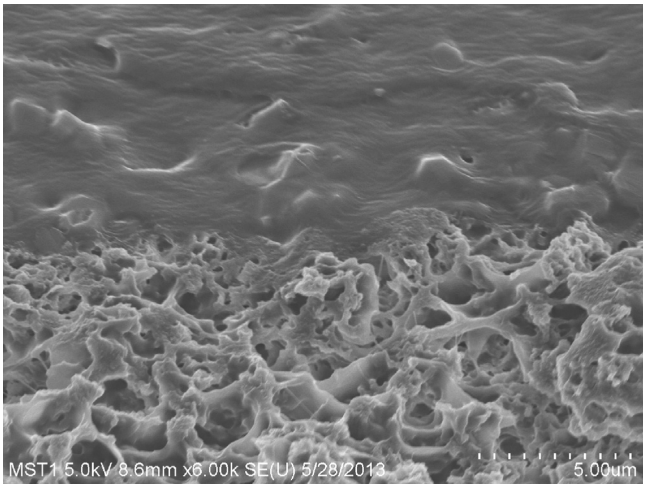

Fig. 9. FESEM image of the cross-section of ZIF-71/PEBA MMMs with ZIF-71 loading of 20 wt% after 100 h continuous PV experiment.

3.4. Comparison of PV performance with literature

Many researches have investigated the recovery of butanol by pervaporation. Table 4 lists the PV performance of various membranes in model ABE solution. The ZIF-71/PEBA mixed matrix membrane with 20 wt% loading in this work has a total flux of

Table 4
Pervaporation performance of different PV membranes in model ABE solution.

Membrane type	T (°C)	Total flux (g/m^2 h)	Separation factor	PSI (g/m^2 h)	Reference
Porous PP	37	10	5	40	[34]
PTFE	40	980	9.5	8330	[35]
HTPB-PU	40	15	11.6[a]	159	[36]
PERVAP-1060	40	340	18.90	6086	[37]
Ceramic supported PDMS	37	993	16.56	15451	[38]
Silicalite-1/PDMS	40	100	50[b]	4900	[39]
OA-POMS liquid membrane	60	55	74	4015	[40]
PEBA	23	41	9.6[b]	352.6	[5]
CNT/PEBA	37	139	18	2363	[41]
ZIF-71/PEBA	37	520	18.8	9256	This work

[a] Evaluated in n-butanol–acetone–water ternary mixtures.

[b] $\beta_{water}^{n-bu\tan ol}$, calculated by the following equation: $\beta_{water}^{n-bu\tan ol} = (Y_{n-bu\tan ol}/Y_{water})/(X_{n-bu\tan ol}/X_{water})$ (Y and X are the weight fractions of components in the permeate and feed, respectively).

520.2 g/m^2 h with the n-butanol separation factor of 18.8 at 37 °C. Compared with the other membranes, the total flux and the separation factor of the MMMs containing ZIF-71 are higher. Simultaneously considering the total flux and n-butanol separation factor for practical application, pervaporation separation index (PSI), which was defined as a measure of separation capability of a membrane and a product of selectivity and flux, was calculated [6]. From Table 4, the ZIF-71/PEBA membrane exhibits quite high PSI and has a great potential application for the biobutanol production.

4. Conclusions

In this study, ZIF-71/PEBA MMMs have been successfully fabricated for biobutanol recovery. A homogeneous dispersion of ZIF-71 particles in the membranes is obtained due to the organic nature of ZIF. The incorporation of ZIF-71 particles into PEBA significantly improves the n-butanol separation performance of the membranes. A simultaneous enhancement in both separation factor and flux has been achieved by optimizing the amount of ZIF-71. The MMMs with 20 wt% loading show high total flux of 520.2 g/m^2 h and n-butanol separation factor of 18.8 at 37 °C in model ABE solution. In addition, the membrane exhibited stable performance in the real ABE fermentation broth for 100 h with average total flux of 447.9 g/m^2 h and n-butanol separation factor of 18.4. The results demonstrate that the ZIF-71/PEBA MMMs can be expected as butanol-selective membranes for industrial production of renewable biofuels.

Acknowledgments

This work was supported by the National Basic Research Program of China (No. 2009CB623406) and the National Natural Science Foundation of China (No. 21176115).

Nomenclature

List of symbols

J	permeation flux (g/m^2 h)
J'	thickness-normalized flux (g/m^2 h)
W	weight of the permeate (g)
A	effective membrane area (m^2)
t	measurement time (h)
l	membrane thickness (μm)
Y_i	weight fractions of component i in permeate
X_i	weight fractions of component i in feed
P	permeability (barrer)
P_i	permeability of component i (barrer)
P_{H_2O}	permeability of water (barrer)
W_i	partial permeate weight of component i (g)
$p_{i,feed}^{vapour}$	equilibrium partial vapor pressure of i in the feed (Pa)
$n_{i,permeate}$	mole fraction of i in the permeate
$p_{permeate}$	permeate pressure (Pa)

Greek letters

α	selectivity
$\alpha_{H_2O}^{i}$	selectivity of component i to water
β	separation factor
β_i	separation factor of component i

References

[1] N. Qureshi, T.C. Ezeji, Butanol, ‘a superior biofuel’ production from agricultural residues (renewable biomass): recent progress in technology, Biofuels Bioprod. Biorefin. 2 (2008) 319–330.

[2] L.M. Vane, A review of pervaporation for product recovery from biomass fermentation processes, J. Chem. Technol. Biotechnol. 80 (2005) 603–629.

[3] X.S. Feng, R.Y.M. Huang, Liquid separation by membrane pervaporation: a review, Ind. Eng. Chem. Res. 36 (1997) 1048–1066.

[4] A. Jonquieres, R. Clement, P. Lochon, J. Neel, M. Dresch, B. Chretien, Industrial state-of-the-art of pervaporation and vapour permeation in the western countries, J. Membr. Sci. 206 (2002) 87–117.

[5] F.F. Liu, L. Liu, X.S. Feng, Separation of acetone–butanol–ethanol (ABE) from dilute aqueous solutions by pervaporation, Sep. Sci. Technol. 42 (2005) 273–282.

[6] E.A. Fouad, X.S. Feng, Use of pervaporation to separate butanol from dilute aqueous solutions: effects of operating conditions and concentration polarization, J. Membr. Sci. 323 (2008) 428–435.

[7] N.L. Le, Y. Wang, T.S. Chung, Pebax/POSS mixed matrix membranes for ethanol recovery from aqueous solutions via pervaporation, J. Membr. Sci. 379 (2011) 174–183.

[8] J. Gu, X. Shi, Y. Bai, H. Zhang, L. Zhang, H. Huang, Silicalite-filled polyether-block-amides membranes for recovering ethanol from aqueous solution by pervaporation, Chem. Eng. Technol. 32 (2009) 155–160.

[9] K.W. Boddeker, G. Bengtson, H. Pingel, Pervaporation of isomeric butanols, J. Membr. Sci. 54 (1990) 1–12.

[10] H.W. Yen, S.F. Lin, I.K. Yang, Use of poly(ether-block-amide) in pervaporation coupling with a fermentor to enhance butanol production in the cultivation of *Clostridium acetobutylicum*, Bioresour. Technol. 133 (2012) 372–377.

[11] X.L. Liu, Y.S. Li, Y. Liu, G.Q. Zhu, J. Liu, W.S. Yang, Capillary supported ultrathin homogeneous silicalite-poly(dimethylsiloxane) nanocomposite membrane for bio-butanol recovery, J. Membr. Sci. 369 (2011) 228–232.

[12] L.M. Vane, V.V. Namboodiri, T.C. Bowen, Hydrophobic zeolite–silicone rubber mixed matrix membranes for ethanol–water separation: effect of zeolite and silicone component selection on pervaporation performance, J. Membr. Sci. 308 (2008) 230–241.

[13] A. Dobrak, A. Figoli, S. Chovau, F. Galiano, S. Simone, I.F.J. Vankelecom, E. Drioli, B. Van der Bruggen, Performance of PDMS membranes in pervaporation: effect of silicalite fillers and comparison with SBS membranes, J. Colloid Interface Sci. 346 (2010) 254–264.

[14] G.P. Liu, F.J. Xiangli, W. Wei, S.N. Liu, W.Q. Jin, Improved performance of PDMS/ceramic composite pervaporation membranes by ZSM-5 homogeneously dispersed in PDMS via a surface graft/coating approach, Chem. Eng. J. 174 (2011) 495–503.

[15] X. Tang, R. Wang, Z. Xiao, E. Shi, J. Yang, Preparation and pervaporation performances of fumed-silica-filled polydimethylsiloxane–polyamide (PA) composite membranes, J. Appl. Polym. Sci. 105 (2007) 3132–3137.

[16] S. Shi, Z. Du, H. Ye, C. Zhang, H. Li, A novel carbon black/polydimethylsiloxane composite membrane with high flux for the separation of ethanol from water by pervaporation, Polymer 38 (2006) 949–955.

[17] J.P. Boom, I.G.M. Punt, H. Zwijnenberg, R. de Boer, D. Bargeman, C.A. Smolders, H. Strathmann, Transport through zeolite filled polymeric membranes, J. Membr. Sci. 138 (1998) 237–258.

[18] J.L.C. Rowsell, O.M. Yaghi, Metal–organic frameworks: a new class of porous materials, Micropor. Mesopor. Mater. 73 (2004) 3–14.

[19] S. Basu, M. Maes, A. Cano-Odena, L. Alaerts, D.E.D. Vos, I.F.J. Vankelecom, Solvent resistant nanofiltration (SRNF) membranes based on metal–organic frameworks, J. Membr. Sci. 344 (2009) 190–198.

[20] M.J.C. Ordonez, K.J. Balkus Jr., J.P. Ferraris, I.H. Musselman, Molecular sieving realized with ZIF-8/Matrimid mixed-matrix membranes, J. Membr. Sci. 361 (2010) 28–37.

[21] T.H. Bae, J.S. Lee, W. Qiu, W.J. Koros, C.W. Jones, S. Nair, A high-performance gas-separation membrane containing submicrometer-sized metal–organic framework crystals, Angew. Chem. Int. Ed. 49 (2010) 9863–9866.

[22] T.X. Yang, Y.C. Xiao, T.S. Chung, Poly-/metal-benzimidazole nano-composite membranes for hydrogen purification, Energy Environ. Sci. 4 (2011) 4171–4180.

[23] X.L. Liu, Y.S. Li, G.Q. Zhu, Y.J. Ban, L.Y. Xu, W.S. Yang, An organophilic pervaporation membrane derived from metal–organic framework nanoparticles for efficient recovery of bio-alcohols, Angew. Chem. Int. Ed. 50 (2011) 10636–10639.

[24] K. Diaz, M. Lopez-Gonzalez, L.F.D. Castillo, E. Riande, Effect of zeolitic imidazolate frameworks on the gas transport performance of ZIF8-poly(1,4-phenylene ether-ether-sulfone) hybrid membranes, J. Membr. Sci. 361 (2011) 206–213.

[25] G.M. Shi, T.X. Yang, T.S. Chung, Polybenzimidazole (PBI)/zeolitic imidazolate frameworks (ZIF-8) mixed matrix membranes for pervaporation dehydration of alcohols, J. Membr. Sci. 415–416 (2012) 577–586.

[26] C.H. Kang, Y.F. Lin, Y.S. Huang, K.L. Tung, K.S. Chang, J.T. Chen, W.S. Huang, K. R. Lee, J.Y. Lai, Synthesis of ZIF-7/chitosan mixed-matrix membranes with improved separation performance of water/ethanol mixtures, J. Membr. Sci. 438 (2013) 105–111.

[27] J.F. Yao, R.Z. Chen, K. Wang, H.T. Wang, Direct synthesis of zeolitic imidazolate framework-8/chitosan composites in chitosan hydrogels, Micropor. Mesopor. Mater. 165 (2013) 200–204.

[28] A. Phan, C.J. Doonan, F.J. Uribe-Romo, C.B. Knobler, M. O'Keeffe, O.M. Yaghi, Synthesis, structure, and carbon dioxide capture properties of zeolitic imidazolate frameworks, Acc. Chem. Res. 43 (2010) 58–67.

[29] A. Nalaparaju, X.S. Zhao, J.W. Jiang, Molecular understanding for the adsorption of water and alcohols in hydrophilic and hydrophobic zeolitic metal–organic frameworks, J. Phys. Chem. C 114 (2010) 11542–11550.

[30] R.P. Lively, M.E. Dose, J.A. Thompson, B.A. McCool, R.R. Chance, W.J. Koros, Ethanol and water adsorption in methanol-derived ZIF-71, Chem. Commun. 47 (2011) 8667–8669.

[31] X.L Dong, Y.S. Lin, Synthesis of organophilic ZIF-71 membrane for pervaporation solvent separation, Chem. Commun. 49 (2013) 1196–1198.

[32] D. Rana, T. Matsuura, Surface modifications for antifouling membranes, Chem. Rev. 110 (2010) 2448–2471.

[33] H.Q. Lin, E.V. Wagner, B.D. Freeman, L.G. Toy, R.P. Gupta, Plasticization-enhanced hydrogen purification using polymeric membranes, Science 311 (2006) 639–642.

[34] N. Qureshi, I.S. Maddox, A. Friedl, Application of continuous substrate feeding to the ABE fermentation: relief of product inhibition using extraction, perstraction, stripping, and pervaporation, Biotechnol. Prog. 8 (1992) 382–390.

[35] D.L. Vrana, M.M. Meagher, J.C. Huang, R.W. Hutkins, B. Duffield, Pervaporation of model acetone–butanol–ethanol fermentation product solutions using polytetrafluoroethene membranes, Sep. Purif. Technol. 28 (1993) 2167–2178.

[36] C.C. Tong, Y.X. Bai, J.P. Wu, L. Zhang, L.R. Yang, J.W. Qian, Pervaporation recovery of acetone-butanol from aqueous solution and fermentation broth using HTPB-based polyurethaneurea membranes, Sep. Sci. Technol. 45 (2010) 751–761.

[37] A. Jonquieres, A. Fane, Filled and unfilled composite GFT PDMS membranes for the recovery of butanols from dilute aqueous solutions: influence of alcohol polarity, J. Membr. Sci. 125 (1997) 245–255.

[38] H. Wu, X.P. Chen, G.P. Liu, M. Jiang, T. Guo, W.Q. Jin, P. Wei, D.W. Zhu, Acetone–butanol–ethanol (ABE) fermentation using Clostridium acetobutylicum XY16 and in situ recovery by PDMS/ceramic composite membrane, Bioprocess Biosyst. Eng. 35 (2012) 1057–1065.

[39] H.L. Zhou, Y. Su, X.R. Chen, Y.H. Wan, Separation of acetone, butanol and ethanol (ABE) from dilute aqueous solutions by silicalite-1/PDMS hybrid pervaporation membranes, Sep. Sci. Technol. 79 (2011) 375–384.

[40] A.B. Beltran, G.M. Nisola, E.L. Vivas, W.H. Cho, W.J. Chung, Poly(octylmethylsiloxane)/oleyl alcohol supported liquid membrane for the pervaporative recovery of 1-butanol from aqueous and ABE model solutions, J. Ind. Eng. Chem. 19 (2013) 182–189.

[41] H.W. Yen, Z.H. Chen, I.K. Yang, Use of the composite membrane of poly(ether-block-amide) and carbon nanotubes (CNTs) in a pervaporation system incorporated with fermentation for butanol production by *Clostridium acetobutylicum*, Bioresour. Technol. 109 (2012) 105–109.